Macromolecules
COMMUNICATION TO THE EDITOR

Macromolecules **2009**, *42*, 3873–3876 **3873**
DOI: 10.1021/ma900444s

Synthesis and Direct Visualization of Electroactive Unimolecular Core−Shell Nanoparticle

Chih-Fu Yeh,[†,‡] **Pei-Ze Huang,**[†,‡] **Woei-Wu Pai,**[‡] **and Leeyih Wang***[,†,‡]

[†]*Institute of Polymer Science and Engineering,*
National Taiwan University, Taipei, Taiwan 106, and
[‡]*Center for Condensed Matter Sciences,*
National Taiwan University, Taipei, Taiwan 106

Received February 27, 2009
Revised Manuscript Received April 20, 2009

Conductive polymers have attracted considerable attention in both academia and industry owing to their unique electrical and optoelectronic characteristics and potential applications in a wide range of areas, such as antistatic agents, electrochromic materials, field-effect transistors, and polymer solar cells.[1] However, many conductive polymers are categorized as rigid, fragile, and intractable materials with limited solubility and processability because of their close-packed conjugated backbone, which substantially limits their industrial application fields.[2] A straightforward method for solving these problems is to blend rigid conjugated polymers with flexible polymers, especially making them as a stable dispersion with a particle structure of nonconjugated core and a conductive shell, to increase the processability, mechanical strength, and transparency of the material.[3] In a solid film, the outer particle layer can easily form a three-dimensional path for charge transport, even with a low loading of conjugated polymers. Therefore, previous studies have demonstrated that these core−shell particles possess a very low conductivity percolation threshold of 3−10 wt %.[4] Such core−shell particles are typically synthesized via oxidative polymerization of conjugated polymers in the presence of polymer latexes stabilized by adsorption of water-soluble polymers, block copolymers, or surfactants. The thickness of an adsorbed stabilizer layer must exceed the thickness of the overlayer of a conjugated polymer on the latex surface to ensure colloidal stability and processability of the final product. However, as the particle size shrinks to the nanoscale, a large amount of stabilizer is needed to generate good stability due to the significant increase in particle surface area. These stabilizers obviously hinder the hopping efficiency of charge between particles. Furthermore, the surfactant may also migrate to the interface between a polymer film and substrate, thus decreasing the adhesion ability of the composite film. This work presents a new approach for preparing stable conductive core−shell nanoparticles without any stabilizer. This method includes construction of a starburst polymer via atom transfer radical polymerization (ATRP)[5] using a multifunctional molecule as a core, followed by growth of conjugated segments from the each chain end of the star polymer to yield a dendritic block copolymer. Atomic force microscopic (AFM) images clearly indicate that these polymers form unimolecular spherical nanoparticles with a well-defined core−shell structure.

Scheme 1 shows the synthetic route of 12-armed poly(*n*-butyl acrylate)-*b*-poly(3-hexylthiophene) (12-PBA-*b*-P3HT). The 12-armed PBA (12-PBA) core was synthesized via ATRP in acetone using a dodecabromo-functionalized molecule and Cu(I)Br/*N*,*N*′,*N*′,*N*′′,*N*′′-pentamethyldiethylenetriamine (PMDETA) as multifunctional initiator and ligand complex, respectively. The gel permeation chromatography (GPC) chromatogram of 12-PBA shows a single symmetric peak with a dispersity index of 1.08 and a number-average molecular weight (M_n) of 18 700, suggestive of a well-controlled process for the growth of each polymer arm in a star during polymerization. As the molecular size of a polymer in a star structure is usually smaller than that in a linear structure, the GPC method frequently underestimates actual molecular weight of a hyperbranched polymer. Therefore, the number-average degree of polymerization (X_n) per arm in 12-PBA was also determined based on the peak area ratio of methyl protons ($\delta = 0.9$ ppm) on side butyl ester chains to peripheral methyl protons ($\delta = 1.1$ ppm) on center initiators in the ^{1}H NMR spectrum of 12-PBA (Figure SI-2). It was calculated to be 17.6, which corresponds to an M_n of 30 200.

The terminal −Br moieties in 12-PBA were modified to generate the same number of hydroxyl groups by nucleophilic substitution using excess ethanolamine as the nucleophile and base. The complete substitution with ethanolamine was verified by the disappearance of the signal $\delta = 4.05$ ppm, corresponding to the proton on the terminal −C*H*Br, and the appearance of two new signals at $\delta = 3.1$ and 3.3 ppm, corresponding to the methylene proton on ethanolamine. Then, the −OH functionalities in the star PBA were esterified with 3-thiopheneacetic acid in CH_2Cl_2 with *N*,*N*′-dicyclohexylcarboimide as the dehydration agent and 4-(dimethylamino)pyridine and *p*-toluenesulfonic acid as reaction promoters to yield thiophene-capped 12-PBA (12-PBA-Th). The average extent of thiophene functionalization was estimated from the area ratio of the methine proton on the thiophene ring ($\delta = 7.20$ ppm) to the peripheral methyl proton on initiators ($\delta = 4.02$ ppm) in the ^{1}H NMR spectrum of 12-PBA-Th (Figure SI-4); it was almost 100%, ensuring the subsequent growth of poly(3-hexylthiophene) from each chain end of 12-PBA. Finally, the synthesis of 12-PBA-*b*-P3HT copolymer was carried out by the oxidative polymerization of 3-hexylthiophene in the presence of 12-PBA-Th using $FeCl_3$ as the oxidant. To reduce the possibility of “free” linear P3HT forming during polymerization, $FeCl_3$ was added to the reaction mixture before 3HT, and the addition of 3HT was kept at a very slow charging rate of 0.1 mL/min to ensure a low monomer concentration. A blank polymerization of 3-hexylthiophene in the absence of 12-PBA-Th was also carried out under the same reaction conditions. GPC data indicated that the thus-prepared poly(3-hexylthiophne) has an M_n and a head-to-tail regioregularity of around 21 000 g mol^{-1} and 73%, respectively, and it has good solubility in hexane. Hence, the as-synthesized crude product was purified by Soxhlet extraction with hexane until a single GPC chromatogram was obtained that completely removed the linear poly(3-hexylthiophene)s not chemically bound on 12-PBA-Th. The disappearance of proton resonance at 7.25 ppm, corresponding to the α-proton of the thiophene ring, provided strong evidence of the growth of P3HT from the terminal thiophene moieties. The monomer ratio of 3-hexylthiophene to *n*-butylacrylate in the as-synthesized starburst block copolymer was approximated based on the integrated area ratio of the thiophene aromatic proton ($\delta = 6.98$ ppm) to the methylene proton next to the carbonyl group in PBA backbone ($\delta = 4.02$ ppm) in the ^{1}H NMR spectrum of 12-PBA-P3HT (Figure 1). It was determined to be 31, which was equivalent to an X_n of 62 for the P3HT block and an M_n of 155 200 for the copolymer.

---

*Corresponding author. E-mail: leewang@ntu.edu.tw.

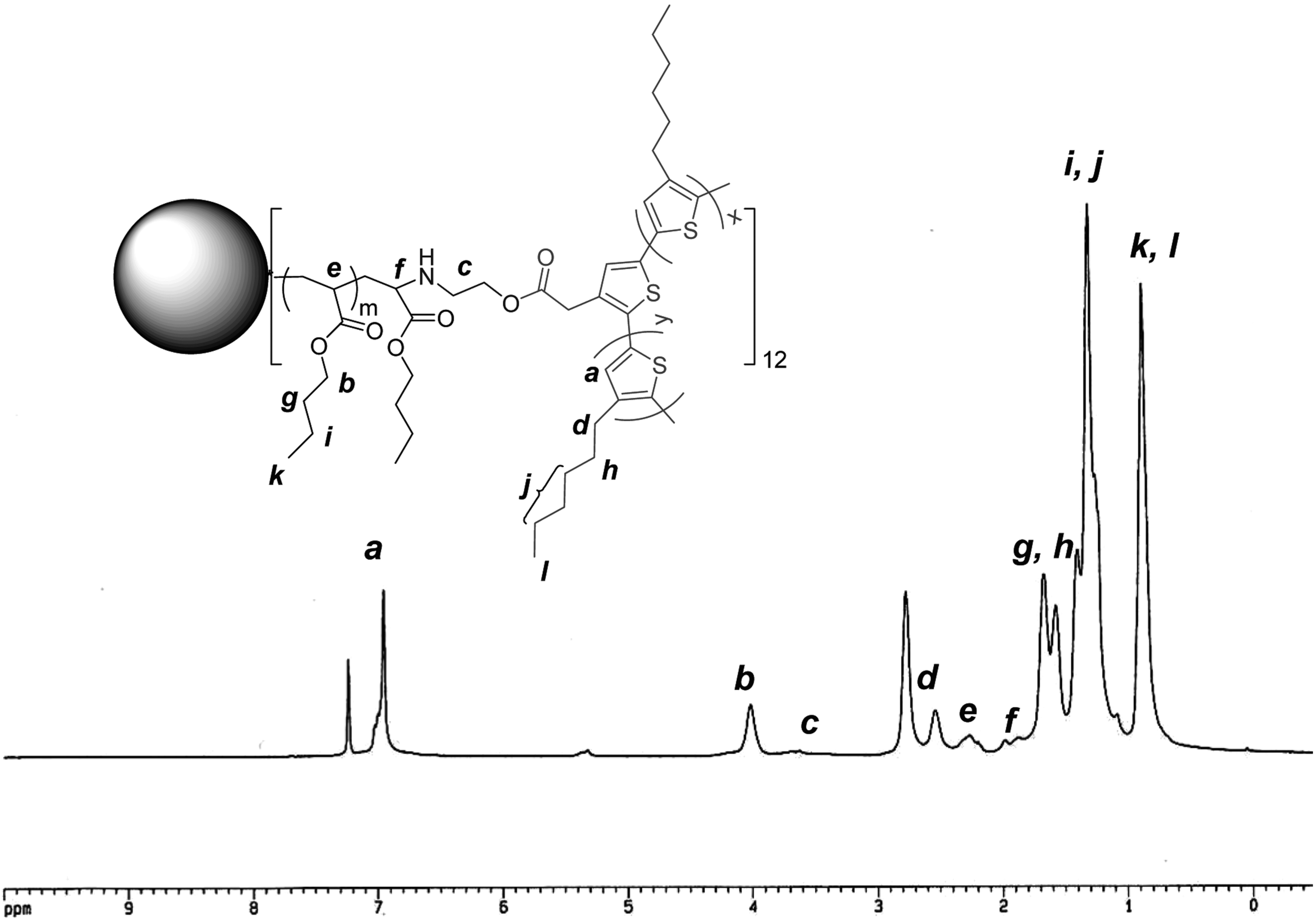

Figure 1. ^{1}H NMR spectrum of 12-armed poly(*n*-butyl acrylate-*b*-3-hexylthiophene). *X* and *Y* represent the number of repeating 3-hexthiophene units from the terminal thiophene moieties, and $m + 1$ stands for the degree of polymerization of *n*-butyl acrylate.

Scheme 1. Synthetic Procedure for Electroactive Unimolecular Core−Shell Nanoparticles

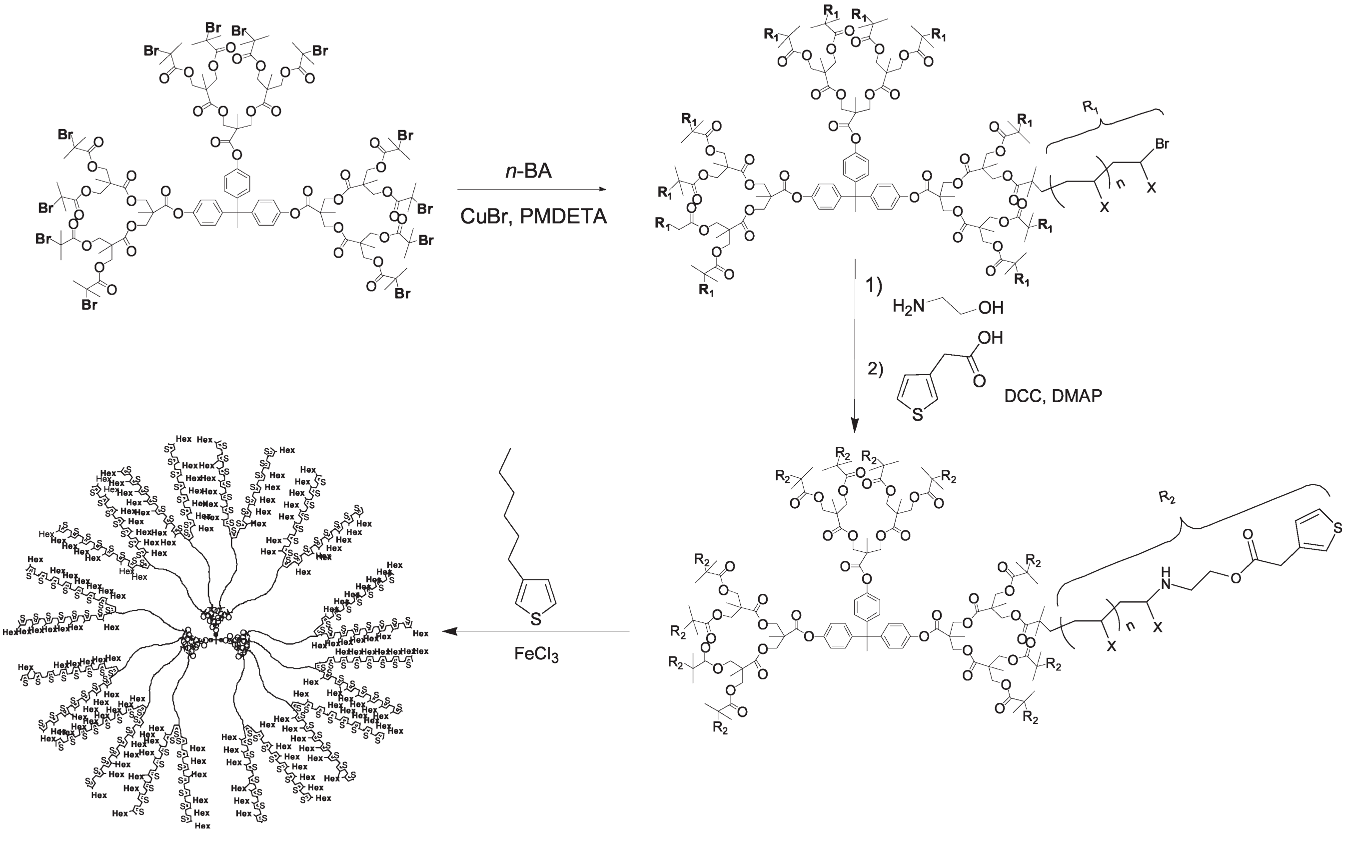

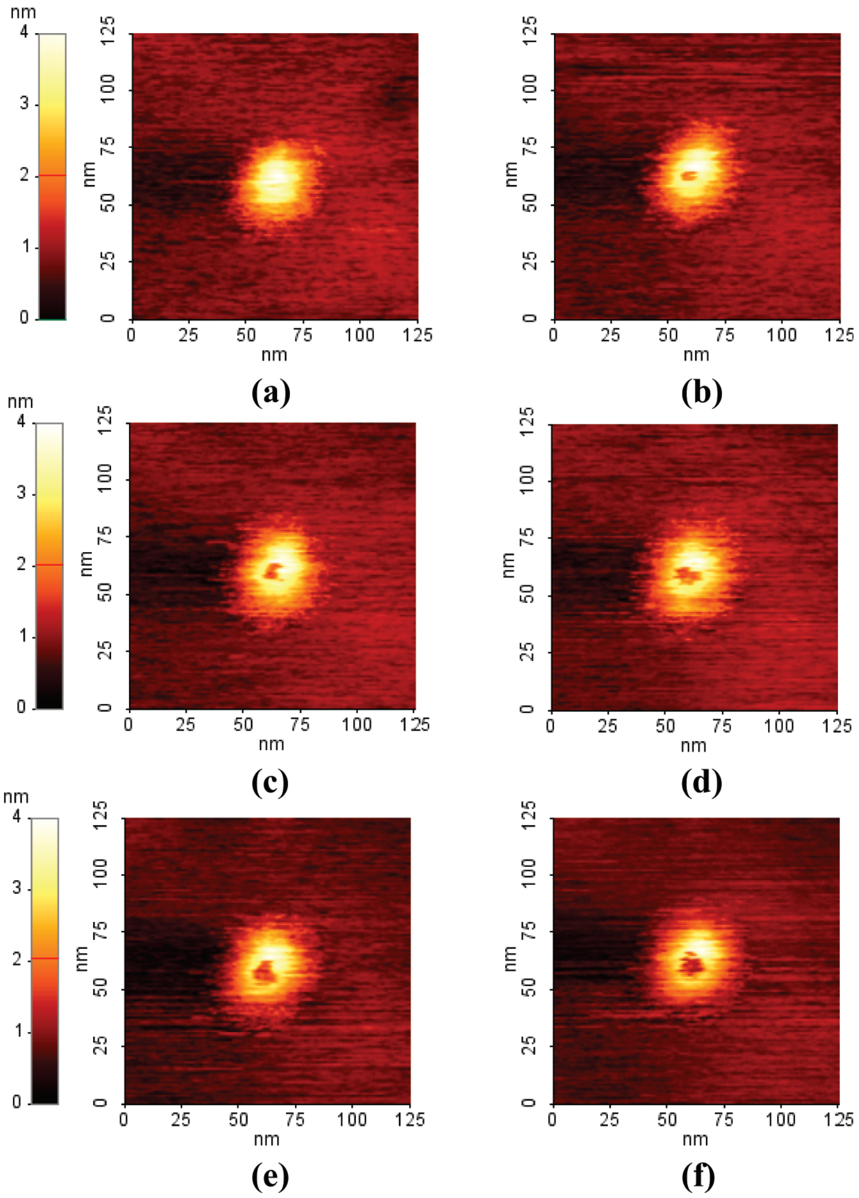

Figure 2. AFM images of an electroactive core–shell nanoparticle with decreased resonance frequency (*f*): (a) 302.51, (b) 302.50, (c) 302.48, (d) 302.46, (e) 302.44, and (f) 302.36 kHz. These frequencies were set by choosing a constant decrement of cantilever amplitude from (a) to (e).

The size and shape of the 12-armed PBA-P3HT block copolymer were examined using an ambient AFM operated in noncontact mode (XE-100, PSIA, Korea). The sample was prepared by dropping an ultradilute 12-PBA-*b*-P3HT/$CHCl_3$ solution (1.33×10^{-10} M) onto a freshly cleaved graphite (1 × 1 cm) and then dried under ambient air. The AFM image (Figure 2a) clearly shows the starburst block copolymer forming a spherical nanoparticle with a diameter of around 28 nm. Moreover, the dynamic light scattering (DLS) data of 12-PBA-*b*-P3HT in $CHCl_3$ exhibited a single and symmetrical size distribution curve with an average diameter of 36 nm and a dispersity index of 0.116 (Figure SI-6). The larger particle size resulted from DLS measurement is because PBA chains are more extended in solution than in solid state, and the measured size is a hydrodynamic diameter. These experimental findings clearly demonstrate that each starburst copolymer formed distinct spherical nanoparticle. Notably, as the probing force of the AFM was increased (with cantilever resonance frequency decreasing from 302.51 to 302.36 kHz), the core region of the particle started to collapse in height (Figure 2b) because the PBA core has a glass transition temperature of roughly −49 °C and can be regarded as a soft and elastomatic material at room temperature. The collapsed area increased and finally formed a donutlike shape (Figure 2c–f). These AFM images provide direct evidence of the formation of a unimolecular nanoparticle of 12-PBA-P3HT with a well-defined soft core and hard conjugated shell.

The UV–vis absorption spectra of the 12-armed polymers in $CHCl_3$ (Figure SI-7) demonstrate that the absorption maximum (λ_{max}) was substantially red-shifted from 289 to 432 nm after oxidative growth of P3HT, suggesting an increase in conjugation length of conjugated segments. The spin-coated 12-PBA-P3HT film on both the glass slide and polyimide was continuous, uniform, and smooth and was peeled away to form a free-standing film with excellent elasticity. The conductivity of the I_2-doped 12-PBA-P3HT film, determined by the conventional four-point probe technique, was 4 mS/cm, which was around 2 orders of magnitude less than that (0.3 S/cm) of I_2-doped pristine P3HT, prepared by oxidative polymerization using $FeCl_3$ as an oxidant in our laboratory, probably because the P3HT chains in the starburst copolymer are shorter than those in the linear structure and less able to be packed in an ordered arrangement. Moreover, bending the 12-PBA-P3HT-coated polyimide back and forth 1000 times had no effect on surface resistivity of the 12-PBA-P3HT film, indicating that incorporating the PBA elastomer into the fragile conjugated material enhanced composite film flexibility and its adhesion to the substrate.

In conclusion, a starburst PBA-*b*-P3HT copolymer with a well-defined chemical structure and molecular weight was synthesized using the core-first (divergent) strategy. The AFM images clearly demonstrate that this block copolymer formed unimolecular spherical nanoparticles with soft cores and hard shells. This new polymer composite particle has the merits of PBA flexibility and the electroactive property of P3HT. The assembly of these unimolecular core−shell nanoparticles into an ordered array is now under development.

Acknowledgment. We thank National Taiwan University and the National Science Council of the Republic of China, Taiwan, for financially supporting this research.

Supporting Information Available: Synthetic details and analyses of this material. This material is available free of charge via the Internet at http://pubs.acs.org.

References and Notes

(1) (a) Das, N. C.; Chaki, T. K.; Khastgir, K.; Chakraborty, A. *Adv. Polym. Technol.* **2001**, *20*, 226–236. (b) Wessling, B. *Synth. Met.* **1998**, *93*, 143–154. (c) Wang, X. H.; Sun, Z. X.; Li, J.; Ye, Z. J.; Jing, X. B.; Wang, F. S. *Synth. Met.* **1999**, *102*, 1377–1380. (d) Li, G.; Jiang, L.; Peng, H. *Macromolecules* **2007**, *40*, 7890–7894. (e) Ma, W.; Kim, J. Y.; Lee, K.; Heeger, A. J. *Macromol. Rapid Commun.* **2007**, *28*, 1776–1780.

(2) (a) Yang, C. Y.; Cao, Y.; Smith, P.; Heeger, A. J. *Synth. Met.* **1993**, *53*, 293–301. (b) Khan, M. A.; Armes, S. P. *Langmuir* **1999**, *15*, 3469–3475.

(3) (a) Khan, M. A.; Armes, S. P. *Adv. Mater.* **2000**, *12*, 671–674. (b) Huijs, F.; Lang, J. *Colloid Polym. Sci.* **2000**, *278*, 746–756.

(4) (a) Wang, L.; Lin, Y.-J.; Chiu, W.-Y. *Synth. Met.* **2001**, *119*, 155–156. (b) Cairns, D. B.; Khan, M. A.; Perruchot, C.; Riede, A.; Armes, S. P. *Chem. Mater.* **2003**, *15*, 233–239. (c) Eisazadeh, H.; Spinks, G.; Wallace, G. G. *Polymer* **1994**, *35*, 3801–3803.

(5) (a) Matyjaszewski, K.; Xia, J. *Chem. Rev.* **2001**, 2921–2990. (b) Kamigaito, M.; Ando, T.; Sawamoto, M. *Chem. Rev.* **2001**, 3689–3746. (c) Gao, H. F.; Matyjaszewski, K. *Macromolecules* **2008**, *41*, 1118–1125. (d) Babin, J.; Lepage, M.; Zhao, Y. *Macromolecules* **2008**, *41*, 1246–1253. (e) Todd, E. M.; Zimmerman, S. C. *J. Am. Chem. Soc.* **2007**, *129*, 14534–14535. (f) High, L. R. H.; Holder, S. J.; Penfold, H. V. *Macromolecules* **2007**, *40*, 7157–7165. (g) Dong, R.; Krishan, S.; Baird, B. A.; Lindau, M.; Ober, C. K. *Biomacromolecules* **2007**, *8*, 3082–3092.